Molecular Cell
Article

The Signaling Adaptor Gab1 Regulates Cell Polarity by Acting as a PAR Protein Scaffold

Ziqiang Yang,[1,*] Bin Xue,[2,3] Masataka Umitsu,[1] Mitsuhiko Ikura,[1,4] Senthil K. Muthuswamy,[1,2,3,4] and Benjamin G. Neel[1,4]
[1]Campbell Family Cancer Research Institute, Ontario Cancer Institute, Princess Margaret Cancer Centre, University Health Network, Toronto, ON M5G 2M9, Canada
[2]Cold Spring Harbor Laboratory, One Bungtown Road, Cold Spring Harbor, NY 11724, USA
[3]Department of Molecular and Cellular Biology, Stony Brook University, Stony Brook, NY 11794, USA
[4]Department of Medical Biophysics, University of Toronto, Toronto, ON M5G 2M9, Canada
*Correspondence: zyang@uhnresearch.ca
http://dx.doi.org/10.1016/j.molcel.2012.06.037

SUMMARY

Cell polarity plays a key role in development and is disrupted in tumors, yet the molecules and mechanisms that regulate polarity remain poorly defined. We found that the scaffolding adaptor GAB1 interacts with two polarity proteins, PAR1 and PAR3. GAB1 binds PAR1 and enhances its kinase activity. GAB1 brings PAR1 and PAR3 into a transient complex, stimulating PAR3 phosphorylation by PAR1. GAB1 and PAR6 bind the PAR3 PDZ1 domain and thereby compete for PAR3 binding. Consequently, *GAB1* depletion causes PAR3 hypophosphorylation and increases PAR3/PAR6 complex formation, resulting in accelerated and enhanced tight junction formation, increased transepithelial resistance, and lateral domain shortening. Conversely, GAB1 overexpression, in a PAR1/PAR3-dependent manner, disrupts epithelial apical-basal polarity, promotes multilumen cyst formation, and enhances growth factor-induced epithelial cell scattering. Our results identify GAB1 as a negative regulator of epithelial cell polarity that functions as a scaffold for modulating PAR protein complexes on the lateral membrane.

INTRODUCTION

Precise control of cell polarity is essential for many biological processes, including asymmetric division of stem/progenitor cells, epithelial morphogenesis, epithelial/mesenchymal transformation (EMT), and cell migration. Disrupted epithelial cell polarity is a hallmark of cancer and contributes to other diseases. Progress has been made in delineating the polarity machinery, but how signaling pathways regulate cell polarity is poorly understood.

Initially identified as the products of *C. elegans* genes whose mutation disrupts asymmetric cell division (Kemphues, 2000), the PAR proteins are essential, highly conserved components of the polarity machinery. Worms have six *par* genes (*par1-par6*): *par1* and *par4* encode protein kinases, *par3* and *par6* encode scaffolding molecules, *par5* encodes a 14-3-3 homolog, and *par2* encodes an E3-ubiquitin ligase-like protein (Macara, 2004b). All of the PAR proteins except PAR2 are found in mammals, where they are indispensable for epithelial development and polarization. *Par3* deletion in mice causes abnormal epicardial development (Hirose et al., 2006). *PAR3* knockdown in MDCK II cells causes the formation of multilumen cysts (Bryant et al., 2010; Hao et al., 2010), delays tight junction (TJ) formation, and decreases transepithelial electrical resistance (TER) in "calcium switch" assays, although TJs eventually do form normally (Chen and Macara, 2005). Although *Par1a* and *Par1b* single knockout mice are viable, compound deletion results in embryonic lethality (Hurov et al., 2007; Lennerz et al., 2010). At the cellular level, *PAR1* depletion causes shortening of the lateral membrane (Cohen et al., 2004; Suzuki et al., 2004), and *PAR1* knockdown cells show increased TER compared with parental cells during polarization (Suzuki et al., 2004). Conversely, but similar to the effects of *PAR3* depletion, *PAR1b* overexpression causes multilumen cysts (Cohen et al., 2011).

The effects of PAR proteins are accompanied, and presumably caused, by their asymmetrical distribution along the apical-basal axis of polarized epithelial cells. PAR3, PAR6, and aPKC are targeted to TJs, where aPKC is activated by GTP-bound CDC42. Similar to the effects of PAR3 deficiency, depletion of *aPKC* also impairs TJ formation (Suzuki et al., 2004). PAR6 and aPKC also localize to the apical domain through interactions with the Crumbs complex (Morais-de-Sá et al., 2010). By contrast, PAR1 resides on the lateral membrane, whereas PAR4 and PAR5 are found mainly in the cytosol. The PAR proteins are responsible, at least in part, for these differences in localization. For example, the PAR3/PAR6/aPKC complex at TJs phosphorylates PAR1, promoting its release into the cytosol and preventing PAR1 from "invading" the TJ from its location on the lateral domain. Conversely, PAR3 is excluded from the lateral domain by PAR1-catalyzed phosphorylation and PAR5-mediated cytosolic translocation (Macara, 2004a, 2004b; Suzuki and Ohno, 2006).

As master regulators of cell polarity, PAR proteins must integrate signals from multiple stimuli. Although the detailed mechanisms remain unclear, the tumor suppressor ASPP2, the receptor tyrosine kinase (RTK) ErbB2, and the Eph family RTK ligand Ephrin B1 modulate polarity via PAR proteins (Aranda et al., 2006; Cong et al., 2010; Lee et al., 2008; Sottocornola

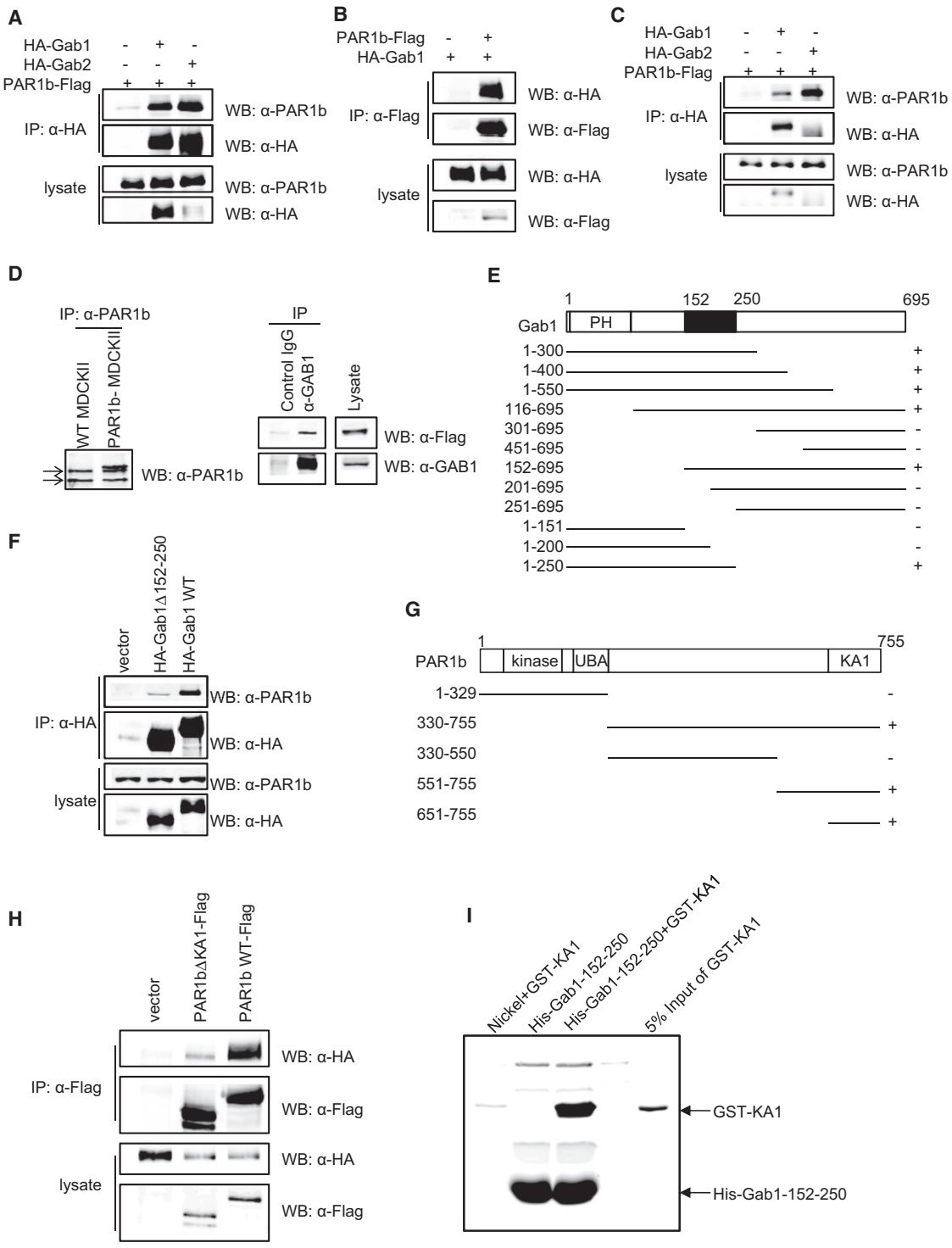

Figure 1. GAB Proteins Associate with PAR1b

(A–C) The indicated expression constructs were cotransfected into 293T (A and B) or MDCK II (C) cells. Lysates were prepared and then immunoprecipitated and immunoblotted with the indicated antibodies.

(D) Left: Lysates from WT MDCK II cells or MDCK II cells stably expressing PAR1b-Flag (PAR1b-MDCK II) were immunoprecipitated and immunoblotted with anti-PAR1b antibodies. Arrows indicate endogenous PAR1b isoforms (Mr ~75 and 80 kDa). Note comparable levels of endogenous PAR1b and expressed PAR1b-Flag. Right: PAR1b-MDCK II lysates were immunoprecipitated with anti-GAB1 antibodies or control IgG, followed by immunoblotting.

(E) Gab1 mutants and their interaction with PAR1b; + indicates binding; −, no interaction.

et al., 2010). Furthermore, CagA (cytotoxin-associated antigen A), a key virulence determinant of *Helicobacter pylori*, the primary cause of gastric ulcers/carcinoma (Hatakeyama, 2004), binds to and inhibits PAR1 and promotes scattering ("hummingbird phenotype") of gastric epithelial cells. This interaction, together with CagA binding and activation of the protein-tyrosine phosphatase SHP2, is thought to contribute to *H. pylori*-induced oncogenesis (Saadat et al., 2007).

CagA is functionally similar to the GAB family (GAB1, GAB2, and GAB3) of scaffolding adaptors (Hatakeyama, 2003), which are critical components of multiple growth factor and cytokine receptor signaling pathways (Gu and Neel, 2003; Wöhrle et al., 2009). Upon agonist stimulation, GABs are recruited to receptors, where they are phosphorylated on multiple tyrosyl residues, creating binding sites for signal relay molecules. For example, tyrosyl phosphorylated GAB1, like CagA, recruits SHP2 and promotes ERK activation. *Gab1* deletion in mice causes embryonic lethality, accompanied by defective skin, liver, and placental development (Itoh et al., 2000; Sachs et al., 2000), some aspects of which could reflect aberrant cell polarity. In MDCK II cells, GAB1 is required for HGF-induced scattering and tubulogenesis (Rosário and Birchmeier, 2003). GAB1 binds to the HGF receptor (Met), and the Met-binding domain of GAB1 and its SHP2 binding sites are essential for HGF-induced scattering and tubulogenesis. GAB1 localizes to epithelial cell-cell contacts via its N-terminal PH domain, and proper subcellular localization is crucial for its role in HGF-induced morphogenesis (Maroun et al., 1999, 2000).

GAB function also is co-opted in several neoplasms. For example, Gab2 is required for BCR/ABL-evoked myeloid transformation (Sattler et al., 2002), whereas GAB2 overexpression accentuates and *Gab2* deficiency impairs Erbb2/Neu-evoked mammary carcinogenesis (Bentires-Alj et al., 2006; Ke et al., 2007). Notably, combining GAB2 overexpression with HER2 (ERBB2) activation in MCF-10A cells results in disruption of their normal gland-like architecture and an invasive "multiacinar" phenotype (Bentires-Alj et al., 2006; Brummer et al., 2006).

Given the similar actions of CagA and GAB1, we asked if GABs also regulate cell polarity via PAR proteins. Indeed, we found that GAB1, like CagA, affects PAR1, but in an entirely different way. Our results identify GAB proteins as key PAR protein scaffolds, which control the dimensions of the lateral membrane of polarized epithelia, the kinetics and extent of TJ formation, and their dissolution during HGF-induced cell scattering.

RESULTS

GAB Proteins Interact with PAR1 Family Members

We first asked if, like CagA (Saadat et al., 2007), GAB proteins bind PAR1. There are three mammalian GABs (GAB1, GAB2, and GAB3) and four PAR1 isoforms (PAR1a–PAR1d). Expression constructs for HA-tagged mouse *Gab1* or *Gab2* and Flag-tagged human *PAR1b* were cotransfected into 293T cells, and after 48 hr, lysates were prepared and immunoprecipitated with anti-HA antibodies. Notably, PAR1b was detected in Gab1 and Gab2 immune complexes (Figure 1A), and Gab1 (or Gab2) was recovered in PAR1b (anti-Flag) immunoprecipitates (Figure 1B and data not shown). Gab1 or Gab2 also coimmunoprecipitated with PAR1a, PAR1c, and PAR1d (data not shown). Moreover, Gab1 (or Gab2) and PAR1b coimmunoprecipitated from lysates of cotransfected MDCK II cells, which (unlike 293 cells) undergo regulated changes in cell polarity (Figure 1C). Using available anti-PAR1 antibodies, we could not detect endogenous PAR1b (or other PAR1 family members) in GAB1 immunoprecipitates from MDCK II cell lysates, so we generated an MDCK II line stably expressing Flag-tagged PAR1b. As expected (Hurov et al., 2001), two endogenous PAR1b isoforms (~75 and 80 kDa, respectively) were detected following immunoprecipitation and immunoblotting with anti-PAR1 antibodies, and Flag-tagged PAR1b was expressed at a similar level to these isoforms (Figure 1D, left panel). Using these cells, we found that GAB1 and PAR1b form a complex when both are expressed at physiological levels (Figure 1D, right panel). Endogenous GAB1/PAR1b interaction also was detected in Caco-2 cells (Figure S1A).

Gab1 Binds the PAR1b KA1 Domain

Using deletion mutants, we defined the region in Gab1 required for interaction with PAR1b (Figure 1E). Expression constructs for HA-tagged versions of these mutants were cotransfected with a PAR1b expression construct, and Gab1/PAR1b association was assessed by anti-HA immunoprecipitation, followed by anti-PAR1b immunoblotting (Figures S1B–S1D). A Gab1 mutant containing only its N-terminal 300 amino acids (Gab1 1–300) interacted with PAR1b (Figure 1E and Figure S1B), while mutants lacking their N-terminal 300 amino acids failed to bind (Figure 1E and Figure S1B). Deleting the PH domain (Gab1 116–695) diminished, but did not abrogate, Gab1/Par1b interaction (Figure 1E and Figure S1B). Thus, PH domain-dependent targeting to an appropriate intracellular location probably is important for Gab1/PAR1b interaction, but amino acids 117–300 of Gab1 contain a second key region for PAR1b interaction. To further define this region, we tested additional Gab1 mutants. Gab1 152–695 bound PAR1b comparably to Gab1 116–695 (Figure 1E and Figure S1C), whereas Gab1 201–695 and Gab1 251–695 lost nearly all binding (Figure 1E and Figure S1C). In parallel, we found that Gab1 1–250 was sufficient for binding PAR1b (Figure S1D). These results suggested that the critical PAR1b binding region lies between Gab1 amino acids 152 and 250, and indeed, deleting this region (Gab1Δ152-250) markedly reduced Gab1/PAR1b interaction (Figure 1F).

(F) The indicated expression constructs were cotransfected into 293T cells, and lysates were immunoprecipitated with anti-HA antibodies and immunoblotted, as indicated.

(G) Diagram of PAR1b mutants and their interaction with Gab1.

(H) The indicated expression constructs were cotransfected into 293T cells, and lysates were immunoprecipitated with M2 beads and immunoblotted, as indicated.

(I) His-Gab1-152-250 immobilized on nickel agarose was incubated with purified GST-KA1, and bound proteins were eluted, resolved by SDS-PAGE, and stained with Coomassie blue. Also, see Figure S1.

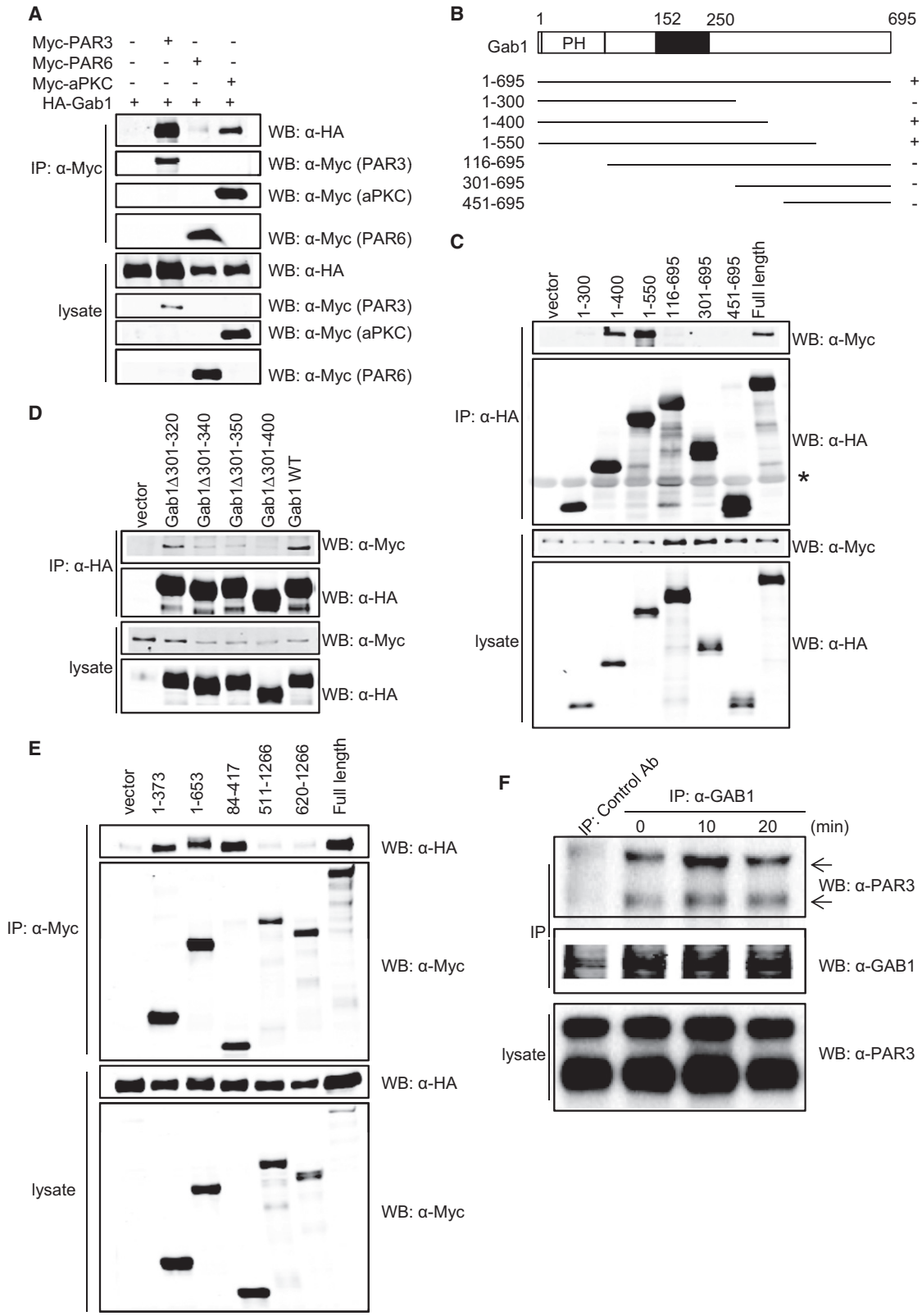
A
Myc-PAR3 - + - -
Myc-PAR6 - - + -
Myc-aPKC - - - +
HA-Gab1 + + + +
IP: α-Myc
WB: α-HA
WB: α-Myc (PAR3)
WB: α-Myc (aPKC)
WB: α-Myc (PAR6)
lysate
WB: α-HA
WB: α-Myc (PAR3)
WB: α-Myc (aPKC)
WB: α-Myc (PAR6)
B
1
152
250
695
Gab1
PH
1-695 +
1-300 -
1-400 +
1-550 +
116-695 -
301-695 -
451-695 -
C
vector
1-300
1-400
1-550
116-695
301-695
451-695
Full length
IP: α-HA
WB: α-Myc
WB: α-HA
*
lysate
WB: α-Myc
WB: α-HA
D
vector
Gab1Δ301-320
Gab1Δ301-340
Gab1Δ301-350
Gab1Δ301-400
Gab1 WT
IP: α-HA
WB: α-Myc
WB: α-HA
lysate
WB: α-Myc
WB: α-HA
E
vector
1-373
1-653
84-417
511-1266
620-1266
Full length
IP: α-Myc
WB: α-HA
WB: α-Myc
WB: α-HA
lysate
WB: α-Myc
F
IP: Control Ab
IP: α-GAB1
0
10
20
(min)
WB: α-PAR3
IP
WB: α-GAB1
lysate
WB: α-PAR3

Next, we mapped the Gab1-binding region on PAR1b. PAR1b contains an N-terminal kinase domain, followed by a UBA (ubiquitin-associated) domain, a long spacer region with aPKC phosphorylation sites, and a C-terminal KA1 (kinase-associated 1) domain. The kinase and UBA domains (PAR1b 1–329) had almost no ability to interact with Gab1 (Figure 1G and Figure S1E), but Par1b constructs containing amino acids 330–755 or 551–755 bound Gab1 even better than WT PAR1b (Figure 1G and Figure S1E), as did a mutant (PAR1b 651–755) containing only the KA1 domain (Figure 1G and Figure S1F). Thus, the KA1 domain is the major binding site for Gab1 and, as expected, a PAR1b mutant lacking its KA1 domain had minimal Gab1 binding (Figure 1H). Notably, the Gab1 binding site on PAR1b (KA1 domain) is distinct from its binding site for CagA (kinase domain; see Discussion). Also, the increased binding of N-terminal truncations of PAR1b to Gab1 suggested that the Gab1 binding site in (full-length) PAR1b might be obscured by interaction between the KA1 and N-terminal domains, a notion confirmed subsequently (see below).

Recently, Pak4 was found to associate with Gab1 (Paliouras et al., 2009) via Gab1 amino acids 116–234, which overlap the PAR1b-binding site (Figure 1E). To ask if Gab1 interacts directly with PAR1b, we carried out in vitro binding assays. Bacterially expressed, His-tagged Gab1 152–250, immobilized on nickel agarose, was incubated with recombinant GST-tagged PAR1b KA1 domain. Bound proteins were recovered by centrifugation, resolved by SDS-PAGE, and detected with Coomassie blue. The KA1 domain of PAR1b bound to Gab1 152–250, indicating that Gab1 and PAR1b can interact directly (Figure 1I).

Gab1 Also Binds PAR3/aPKC

We next asked if Gab1 interacts with other PAR proteins. Indeed, transiently expressed HA-Gab1 coimmunoprecipitated with transiently expressed Myc-PAR3 and Myc-aPKC; by contrast, there was minimal HA-Gab1 association with Myc-PAR6, though the latter was expressed at higher levels than PAR3 (Figure 2A). Cotransfection of PAR3 significantly enhanced aPKC interaction with Gab1 (Figure S2A), suggesting that aPKC binds Gab1 at least in part via PAR3 (see below).

We then mapped the region on Gab1 required for PAR3 association. Deleting the PH domain (Gab1 116–695) abrogated Gab1 interaction with PAR3 (Figures 2B and 2C). The N-terminal 300 amino acids of Gab1 (1–300), which are sufficient for PAR1b binding, did not bind PAR3, indicating that the PAR1 and PAR3 binding sites are distinct. However, extending this fragment to include the N-terminal 400 amino acids (Gab1 1–400) restored PAR3 interaction (Figures 2B and 2C). Hence, a second key region for PAR3 binding (in addition to the Gab1 PH domain) lies between amino acids 300 and 400 (Figures 2B and 2C). Gab1 lacking this region (Gab1Δ301–400) did not coimmunoprecipitate with PAR3, while internal deletions within this region decreased, but did not eliminate, Gab1/PAR3 interaction (Figure 2D). We therefore define amino acids 301–400 of Gab1 as the PAR3-binding site. Consistent with the results of the PAR3/aPKC cotransfection experiments (Figure S2A), Gab1Δ301–400 and Gab1Δ301–340 also showed decreased interaction with aPKC (Figure S2B).

PAR3 contains three PDZ domains through which it interacts with multiple proteins. PAR3 fragments containing the PDZ1 domain (1–373, 1–653, and 84–417) interacted with Gab1; conversely, fragments lacking this domain failed to interact (Figure 2E and Figure S2C). Moreover, recombinant PAR3 PDZ1 domain (expressed as a GST fusion protein) interacted with transiently expressed HA-Gab1 (Figure S2D), indicating that the PAR3 PDZ1 domain is necessary and sufficient for interaction with Gab1. GAB1 also coimmunoprecipitated with PAR3 in lysates from MDCK II or MCF-10A mammary epithelial cells (Figure 2F and Figure S2E), and this interaction increased following activation of coexpressed rat Erbb2/Neu (see Discussion).

Gab1 Acts as a Scaffold to Facilitate PAR3 Phosphorylation by PAR1

Because Gab1 uses different regions to interact with PAR1 and PAR3, respectively, it might function as a scaffold to bring together these two polarity regulators. To test this possibility, we cotransfected 293T cells with expression constructs for Myc-tagged *PAR3*, Flag-tagged *PAR1b*, and/or HA-tagged *Gab1*. After 48 hr, lysates were prepared, PAR3 was immunoprecipitated with anti-Myc antibodies, and coprecipitating PAR1b or Gab1 was detected with anti-PAR1b or anti-HA antibodies, respectively. Indeed, Gab1 coexpression increased the amount of PAR1b recovered in PAR3 immunoprecipitates (Figure 3A).

We noticed that less Gab1 coimmunoprecipitated with PAR3 when *Gab1*, *PAR1*, and *PAR3* were coexpressed (Figure 3A) than when *Gab1* and *PAR3* were cotransfected (Figure 2A). These findings suggested that PAR1b might inhibit the interaction of Gab1 with PAR3. We compared the interaction of Gab1 and PAR3 with or without coexpressed PAR1b, and indeed, less Gab1/PAR3 complex was detected in the presence of PAR1b. By contrast, a PAR1b point mutant without kinase activity (PAR1b(D160N)) did not decrease the Gab1/PAR3 complex (Figure 3B). When PAR3 diffuses from TJs into the lateral membranes of polarized epithelial cells, it is phosphorylated by PAR1 and then released into the cytosol; thus, PAR1-catalyzed PAR3

Figure 2. Gab1 Binds to the PDZ1 Domain of PAR3

(A) The indicated expression constructs were cotransfected into 293T cells, and lysates were immunoprecipitated with anti-Myc antibodies and immunoblotted, as indicated.

(B) Gab1 mutants and their interactions with PAR3; + indicates binding; −, no interaction.

(C and D) The indicated constructs were cotransfected into 293T cells, and lysates were immunoprecipitated with anti-HA antibodies and immunoblotted, as indicated. * indicates IgG heavy chain.

(E) The indicated constructs were cotransfected into 293T cells, and lysates were immunoprecipitated with anti-Myc antibodies and immunoblotted, as indicated.

(F) MDCK II/ErbB2 cells, which express ErbB2 fused to FKBP (Aranda et al., 2006), were stimulated with AP1510 (1 μM) as indicated, and anti-GST (Control Ab) or anti-GAB1 immunoprecipitates were prepared and immunoblotted. Arrows indicate PAR3 isoforms (150 kDa and 180 kDa) that coprecipitate with GAB1. Also, see Figure S2.

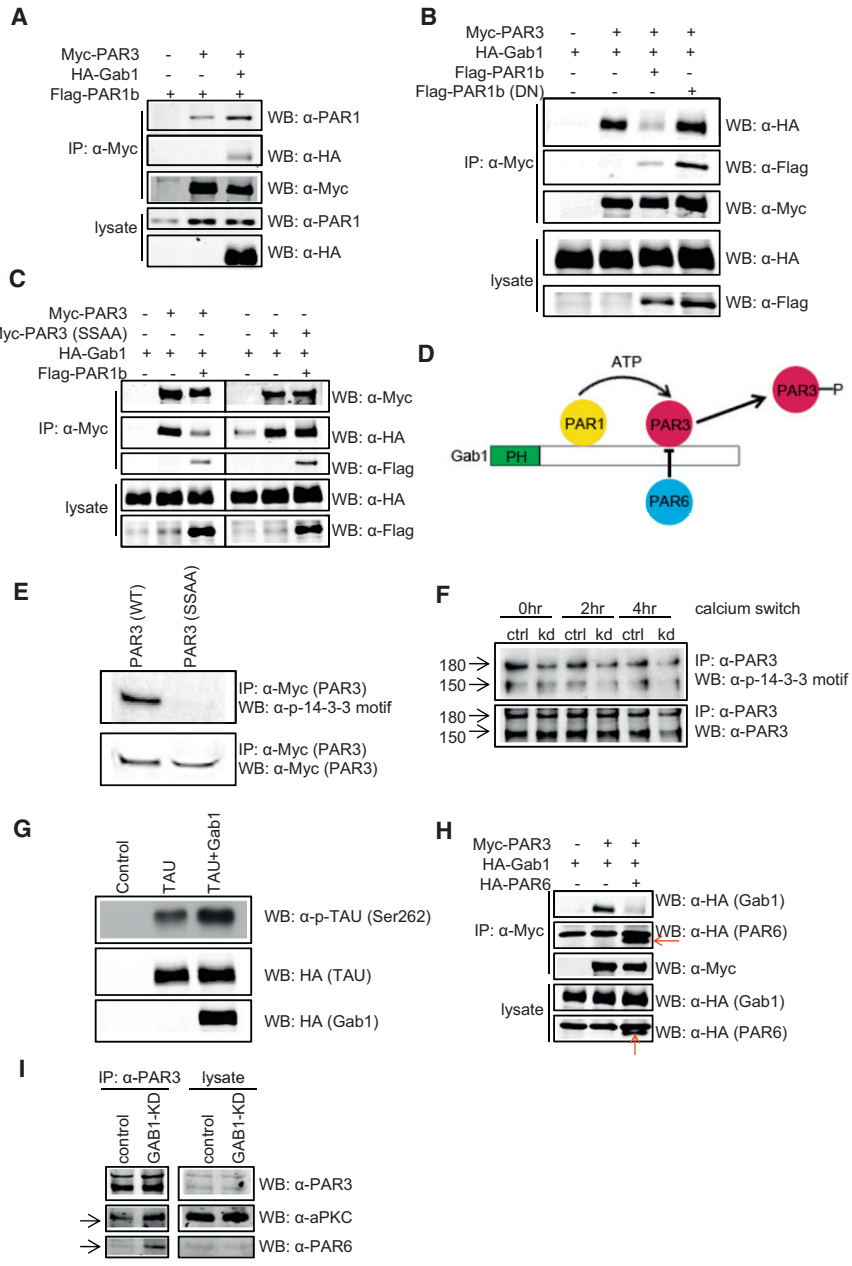

Figure 3. Gab1 Acts as a Scaffold to Facilitate PAR3 Phosphorylation by PAR1

(A) Gab1 promotes PAR3/PAR1 interaction. The indicated constructs were cotransfected into 293T cells, and Myc-PAR3/PAR1-Flag interaction was assessed.

(B) PAR1b, via its kinase activity, disrupts PAR3 interaction with Gab1. The indicated constructs were cotransfected into 293T cells, and Myc-PAR3/HA-Gab1 interaction was assessed.

(C) PAR1b disrupts Gab1/PAR3 interaction by phosphorylating PAR3. The indicated constructs were cotransfected into 293T cells. The effect of PAR1b-Flag expression on HA-Gab1/ Myc-PAR3 (or Myc-PAR3 [SSAA]) interaction was compared by immunoblotting.

(D) Model of Gab1/PAR protein interactions (see text for details).

(E) MDCK II cells were transiently transfected with the indicated constructs, and PAR3 phosphorylation was analyzed by immunoprecipitation/immunoblotting with anti-p-14-3-3 motif antibodies. Note specificity of the latter.

(F) PAR3 phosphorylation by PAR1 in Control or *GAB1*-KD MDCK II cells undergoing calcium switch.

(G) Gab1 enhances PAR1b kinase activity. *HA-TAU* alone or with *HA-Gab1* was transfected into *GAB1*-KD MDCK II cells stably expressing PAR1b. TAU phosphorylation was assessed by immunoblotting.

(H) PAR6 inhibits Gab1/PAR3 interaction. The indicated constructs were cotransfected into 293T cells, and Myc-PAR3/HA-Gab1 interaction was assessed. Red arrows indicate HA-PAR6; the band above is nonspecific.

(I) Control or *GAB1*-KD MDCK II lysates were immunoprecipitated with anti-PAR3 antibodies, and coprecipitating PAR6 and aPKC (arrows) were detected by immunoblotting. Also, see Figure S3.

phosphorylation acts to restrict PAR3 to TJs (Benton and St Johnston, 2003; Hurd et al., 2003). We therefore asked whether PAR1b affected the interaction of Gab1 with a phosphorylation-resistant mutant of PAR3 (PAR3 S144A/S873A). Notably, Gab1 coimmunoprecipitation with phosphorylation-resistant PAR3 (SSAA) was unaffected by PAR1 (Figure 3C), indicating that PAR1b disrupts Gab1/PAR3 interaction, at least in part, by phosphorylating PAR3.

Taken together, these results suggested that Gab1 brings together PAR3 and PAR1 to facilitate PAR3 phosphorylation (Figure 3D). To test this hypothesis further, we depleted *GAB1* in MDCK II cells (Figure S3A) and monitored PAR3 phosphorylation during a calcium switch assay by immunoblotting PAR3 immunoprecipitates with an anti-phospho-14-3-3 motif antibody. Notably, this antibody fails to recognize a PAR3 mutant lacking its PAR1b phosphorylation sites, S144/873 (Figure 3E). As predicted, PAR3 phosphorylation was decreased in *GAB1*-knockdown (*GAB1*-KD) cells compared with controls (Figure 3F). Hence, GAB1, by facilitating PAR1/PAR3 interaction, maintains normal levels of PAR3 phosphorylation during cell polarization. Consistent with this idea, re-expressing Gab1 in *GAB1*-KD cells (by using a mouse *Gab1* cDNA resistant to the canine shRNA) enhanced PAR3 phosphorylation. By contrast, Gab1 mutants lacking their PAR1b-binding or PAR3-binding sites were less efficient in restoring PAR3 phosphorylation during a calcium switch (Figure S3B).

Gab1 Enhances PAR1 Kinase Activity

The kinase activity of the yeast PAR1 homologs, Kin1p/Kin2p, is autoinhibited by intramolecular interaction of their C termini and N-terminal kinase domains (Elbert et al., 2005), so we asked if the

C-terminal KA1 domain of PAR1b also interacted with its N terminus. Lysates of 293T cells transiently expressing PAR1b (1–650) were incubated with purified, recombinant GST-tagged KA1 domain. Bound proteins were recovered on glutathione-agarose and analyzed by immunoblotting (Figure S3C). As reported for Kin1p/Kin2p, the N-terminal part of human PAR1b, containing the kinase domain, interacted (in *trans*) with the C-terminal KA1 domain. This interaction was inhibited by adding increasing amounts of lysate from 293T cells transiently expressing Gab1, but not by parental 293T lysate (Figure S3C). These findings suggested that Gab1, by binding to the PAR1 KA1 domain and disrupting its interaction with the kinase domain, might stimulate PAR1; indeed, TAU phosphorylation by PAR1b was enhanced by Gab1 overexpression (Figure 3G). Thus, Gab1 promotes PAR1 phosphorylation of PAR3 in two ways: it facilitates PAR1/PAR3 colocalization and increases PAR1 kinase activity by relieving autoinhibition.

Gab1 Regulates the Amount of the PAR3-PAR6-aPKC Complex

When epithelial cells polarize, PAR3, PAR6, and aPKC form a complex. PAR3 interaction with PAR6 is mediated by the PAR3 PDZ1 domain (Macara, 2004b). Because Gab1 also binds to this domain (Figure 2E), and Gab1 forms a complex with PAR3, but not with PAR6 (Figure 2A), we suspected that Gab1 and PAR6 might compete for binding to PAR3. Indeed, coexpression of PAR6 inhibited the interaction of transiently expressed PAR3 and Gab1 (Figure 3H). Furthermore, more endogenous PAR6 coimmunoprecipitated with PAR3 from lysates of *GAB1*-KD MDCK II cells than from controls. We also detected more PAR3-aPKC complex in *GAB1*-KD cells, consistent with increased PAR3-PAR6 interaction (Figure 3I, arrows), and these cells formed more PAR3/PAR6/aPKC complex during a calcium switch (Figure S3D). Therefore, GAB1 also controls the amount of PAR3/aPKC/PAR6 complex in two ways: first, it competes directly with PAR6 for binding to PAR3 (Figure 3D) and second, it promotes PAR1 phosphorylation of PAR3, releasing PAR3 from the membrane and limiting its access to PAR6.

GAB1 Regulates TJ Formation and Function

Given the ability of Gab1 to regulate PAR1 activity, PAR3 phosphorylation, and PAR6/PAR3 interaction, we hypothesized that GAB1, like the PAR proteins, is important for cell polarity control. To explore this possibility, we first compared TJ formation in control and *GAB1*-KD MDCK II cells subjected to a calcium switch assay. As expected, TJs, as assessed by immunofluorescence staining for ZO-1, were disrupted in control and *GAB1*-KD MDCK II cells placed in calcium-free media (Figure 4A). Upon readdition of calcium, TJs began to form at cell-cell contacts. In *GAB1*-KD cells, ZO-1 began to accumulate as early as 15 min after calcium repletion and formed a complete, honeycomb-like structure by 1 hr. By contrast, in controls, interruptions in the pattern of ZO-1 staining persisted for > 1 hr (Figure 4A). In addition, PAR3 accumulated much faster at cell-cell contacts in *GAB1*-KD cells (Figure S4A), and *GAB1* depletion in human Caco-2 colonic epithelial cells also enhanced TJ formation (Figure S4B). Gab1 distributed throughout the cell in calcium-depleted cells, but accumulated rapidly at cell-cell contacts upon calcium repletion (Figure 4C), placing it in an appropriate location to regulate TJ formation. A key function of GAB1 is to bind SHP2 and promote RAS/ERK activation in response to growth factor stimulation. However, addition of the MEK inhibitor U0126 did not affect TJ formation in control or *GAB1*-KD MDCK II cells (data not shown).

To assess the integrity of the TJs in *GAB1*-KD cells (and to provide independent, quantitative validation of the effects of GAB1 deficiency on TJ formation), we measured TER. In calcium-free medium, TER was close to zero in control and *GAB1*-KD cells, indicating disrupted TJs. When calcium was repleted, TER increased in control and *GAB1*-KD cells, but *GAB1*-KD cells attained a higher TER at a faster rate than did controls (Figure 4B), consistent with their more rapid TJ formation (Figure 4A).

Gab1 Regulates TJ Function by Binding to PAR Proteins

To confirm that precocious TJ formation in *GAB1*-KD cells reflected GAB1 deficiency rather than off-target effects, we re-expressed Gab1 (Figure 5A). Gab1 (pSp-shGab1 + pBabe-Gab1) decreased the rate of TJ formation compared with control vector-reconstituted cells (pSp-shGab1 + pBabe) (Figure 5B). Unfortunately, using this vector system, Gab1 was substantially overexpressed, and we were unable to find an expression system that resulted in re-expression of Gab1 to near-endogenous levels. Nevertheless, reconstituting *GAB1*-KD MDCK II cells with Gab1 mutants lacking their PAR1b (pSp-shGab1 + pBabe-Gab1Δ152-250) or PAR3 (pSp-shGab1 + pBabe-Gab1Δ301-400) binding sites did not affect TJ formation. By contrast, a Gab1 mutant lacking its CRK-binding sites, two of which overlap the PAR3 binding site, was as competent as WT (wild-type) Gab1 in delaying TJ formation (Figure 5B).

Because the Pak4-binding site on Gab1 (Paliouras et al., 2009) overlaps the PAR1b-binding site, we took two approaches to assess the effects of Gab1/PAR1 complex formation directly. First, we fused Gab1Δ152-250 to PAR1b via a flexible linker (Figure S5A). We also generated a Gab1 mutant that can associate inducibly with PAR1b by fusing the Gab1Δ152-250 C terminus to FKBP and the PAR1b C terminus to a modified FRB (F*RB) peptide (Figure S5B). The direct fusion of Gab1Δ152-250 and PAR1b (pSp-shGab1 + pBabe-Gab1Δ152-250-PAR1b) was as effective as WT Gab1 in delaying TJ formation (Figure 5B), even though it was expressed at much lower (and near endogenous GAB1) levels (Figure 5A). Similarly, inducing Gab1Δ152-250-FKBP association with PAR1b-F*RB in *GAB1*-KD MDCK II cells, by treatment with the rapamycin analog AP21697 (dimerizer), delayed TJ formation (Figure 5D).

We also monitored TER development in *GAB1*-KD and -reconstituted MDCK II cells. Consistent with their effects on TJ formation, expressing WT Gab1 (KD + Gab1) or the direct Gab1Δ152-250-PAR1b fusion protein (KD + fusion) lowered TER in *GAB1*-KD MDCK II cells. By contrast, the control vector (KD + V), PAR1b-binding mutant (KD + Δ152-250), and PAR3-binding mutant (KD + Δ301–400) were defective in this assay (Figure 5C). AP21697-induced dimerization of Gab1Δ152-250-FKBP and PAR1b-F*RB also lowered TER (Figure 5E). We conclude that precocious TJ formation and TER establishment

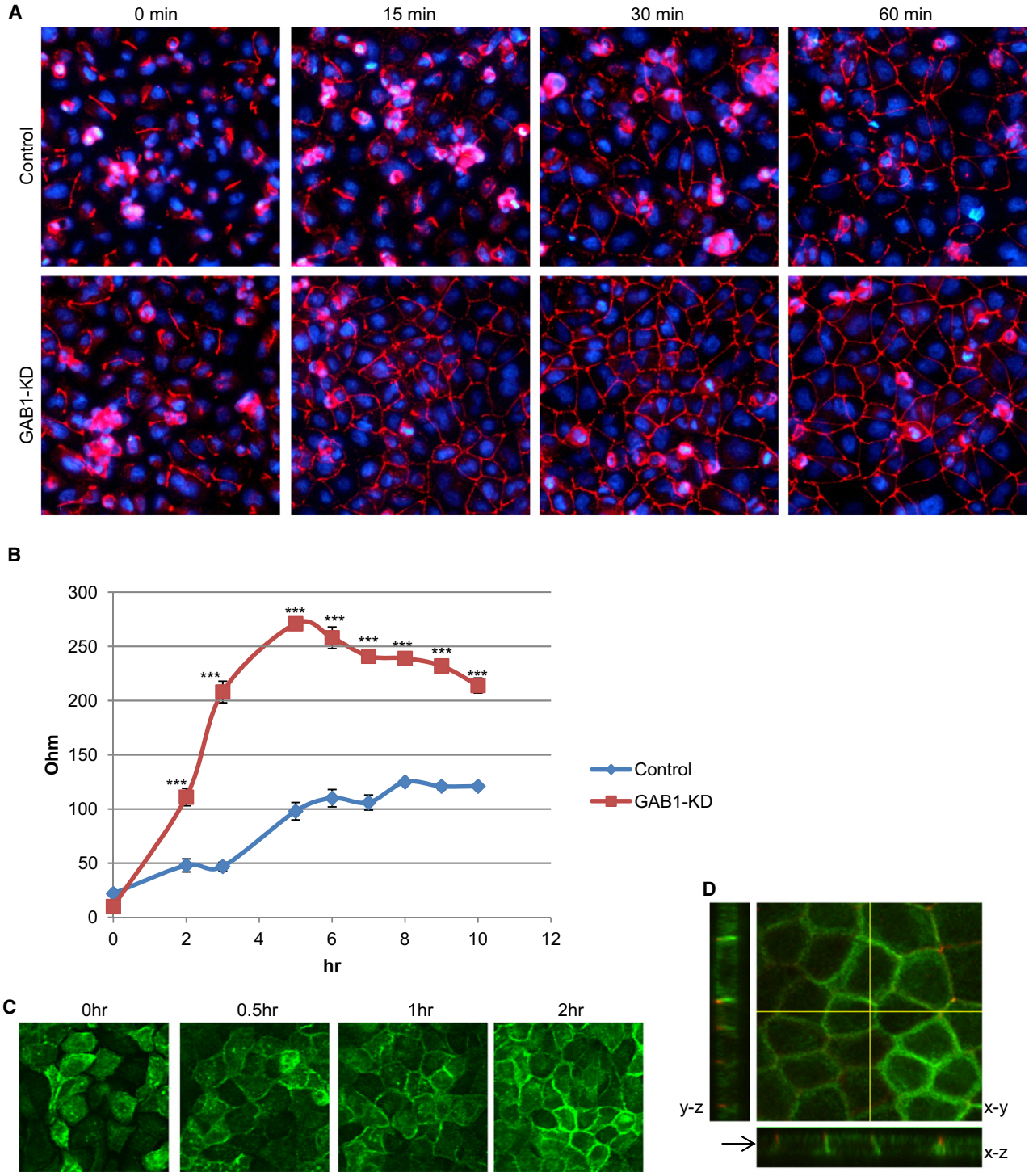

Figure 4. GAB1 Regulates TJ Formation/Function

(A) Calcium switch assays. Control and *GAB1*-KD MDCK II cells were fixed at the indicated times after Ca^{2+} repletion and immunostained for ZO-1. Nuclei were stained with DAPI. Representative fluorescent images are shown.

(B) TER (mean ± SD) in control and *GAB1*-KD MDCK II cells following calcium switch (***$p < 0.001$).

(C) MDCK II cells stably expressing HA-Gab1 undergoing calcium switch were stained with anti-HA antibody to visualize Gab1. Note that Gab1 resides in the cytosol when cells are in Ca^{2+}-free medium, but accumulates at cell-cell contacts upon calcium switch.

(D) MDCK II-HA-Gab1 cells grown on filters for 24 hr were immunostained with anti-HA (green) and anti-ZO-1 (red). Gab1 resides on the lateral membrane, whereas ZO-1 is on tight junctions. Representative x-y, x-z, and y-z slices are shown. Arrow indicates position of x-y plane in the x-z axis. Also, see Figure S4.

in *GAB1*-KD MDCK II cells is due to loss of GAB1 and, more specifically, its interactions with PAR1b and PAR3.

GAB1/PAR Complexes Regulate Apical-Basal Polarity

In polarized epithelia, the cell membrane is divided into apical and lateral domains. GAB1, like PAR1, localized to the lateral domain of MDCK II cells (Figure 4D). Previous studies showed that PAR1 depletion (by RNAi) results in shortening of the lateral membrane (Cohen et al., 2004; Suzuki et al., 2004). Because GAB1 and PAR1 form a complex and GAB1 enhances PAR1 activity, we assessed the effect of GAB1 on apical-basal polarity. Control and *GAB1*-KD MDCK II cells were cultured on porous filters for 3 days and then immunostained with anti-ZO-1, anti-E-cadherin, and anti-gp135 antibodies. Notably, the lateral membrane (E-cadherin stain) was shortened in *GAB1*-KD MDCK II cells compared with controls (Figure 6A and Figure S6B), providing further evidence of the functional importance of GAB1/PAR1 interaction. GAB1 depletion also increased the thickness of TJs (i.e., the fraction of the membrane occupied by TJs) without affecting overall cell polarization, as shown by normal apical marker staining (Figure 6B).

We next analyzed cells re-expressing WT Gab1 or its PAR1- or PAR3-binding deficient mutants. As noted above (Figure 5), these Gab proteins were overexpressed in reconstituted cells, and Gab1 overexpression caused a severe loss of polarity: ZO-1 diffused to the basolateral domain and cells lost their typical cobblestone morphology (Figure 6C). By contrast, ZO-1 and E-cadherin remained well-segregated in cells expressing the PAR1b- or PAR3-binding site mutants (Figure 6C and Figure S6C). Cells (over)expressing WT Gab1 also displayed a wavy apical surface as shown by gp135 staining, while PAR1b- or PAR3-binding deficient mutant-expressing cells retained an even apical surface (Figure S6A). Thus, GAB1 overexpression disrupts apical-basal polarity in a PAR1b- and PAR3-dependent manner.

MDCK II cells form single-lumen cysts when cultured in Matrigel, and PAR3 depletion causes multilumen cysts due to abnormal spindle orientation (Bryant et al., 2010; Hao et al., 2010). Our data indicated that Gab1 overexpression negatively regulates PAR3 by increasing its phosphorylation by PAR1. Indeed, MDCK II cells expressing WT Gab1 formed cysts with multiple lumens (Figure 6D and Figure S6D). Moreover, cells within these cysts had disrupted apical-basal polarity (as shown by the presence of multiple ZO-1-positive domains), although most cells on the outer surface of the cysts retained normal apical-basal polarity with distinct, properly ordered TJs (ZO-1 stain) and lateral membranes (β-catenin stain) (Figure S6E). By contrast, cells expressing Gab1 mutants lacking PAR1b- or PAR3-binding sites formed single-lumen cysts, providing further evidence that GAB1 controls cell polarity by regulating PAR1 and PAR3.

GAB1/PAR Complexes Regulate Cell Scattering

Growth factors can promote the disruption of cell junctions and the conversion of polarized epithelia to motile cells with a mesenchymal phenotype, a process termed "cell scattering." Gab1 overexpression sensitizes MDCK II cells to HGF-induced scattering via Gab1/SHP2 and Gab1/Pak4 interactions (Paliouras et al., 2009). We wondered whether Gab1/PAR interactions also might be important. Indeed, overexpression of WT Gab1 promoted scattering even in the absence of HGF, whereas scattering in response to an HGF dose (1 ng/ml) that does not promote scattering of WT cells (Figure 7A, leftmost panels) was potentiated by Gab1 expression (Figure 7A, pSp-shGab1 + pBabe-Gab1, and Figure S7A). By contrast, vector control (pSp-shGab1 + pBabe)-, Gab1Δ152-250 (pSp-shGab1 + pBabe-Gab1Δ152-250)-, or Gab1Δ301-400 (pSp-shGab1 + pBabe-GAB1Δ301-400)-reconstituted cells largely remained in tight epithelioid colonies (Figure 7A and Figure S7A). These data indicate that the ability of Gab1 to promote cell scattering is impaired by deletion of its PAR1b- or PAR3-binding sites. Finally, forced dimerization of Gab1Δ152-250-FKBP and PAR1b-F*RB in *GAB1*-KD MDCK II cells restored HGF-evoked scattering (Figure 7B and Figure S7B), confirming that Gab1/PAR1b interaction is required for this process.

DISCUSSION

During development, epithelial cells polarize and assemble into complex structures, directed, in part, by growth factor and cytokine signaling. These processes are disrupted in many diseases, including cancer, yet how signaling pathways impact the polarity machinery has largely remained elusive. We uncovered a role for GAB proteins, conserved scaffolding adaptors that play essential roles in growth factor/cytokine signaling from worms to humans, in regulating polarity via PAR proteins. GAB proteins regulate epithelial cell scattering and morphogenesis (Rosário and Birchmeier, 2003), but heretofore, these effects have been attributed to their ability to recruit and activate SH2 domain-containing signal relay molecules (e.g., SHP2, PI3K). The finding that *H. pylori* CagA, which co-opts GAB protein functions and binds and inhibits PAR1 (Saadat et al., 2007), raised the possibility that GAB proteins have similar effects. Indeed, GAB1 interacts with the polarity machinery, but in an entirely different way. Our studies reveal a general role for GAB1 (and probably other GAB proteins) as a protein scaffold that facilitates mutual exclusion of PAR complexes from TJs and the lateral membranes, respectively, of polarized epithelial cells. As GAB proteins are implicated in several malignancies, our findings also have implications for understanding how polarity is disrupted in cancer.

Gab1, like CagA, binds to PAR1b (and other PAR1 isoforms). But whereas CagA binds and inhibits the PAR1 kinase domain (Saadat et al., 2007), Gab1 binds the KA1 domain (Figures 1G and 1H and Figures S1E and S1F). In yeast PAR1 orthologs, the KA1 domain, via an intramolecular interaction, inhibits kinase activity (Elbert et al., 2005). Similarly, Gab1 binding to PAR1 disrupts KA1/kinase domain interactions in mammalian cells (Figure S3C). Gab1 expression also enhances the phosphorylation of the PAR1 substrate TAU (Figure 3G), indicating that Gab1 activates PAR1 in vivo.

Also unlike CagA, we found that Gab1 interacts with PAR3 (Figure 2A). The PAR1 and PAR3 binding sites on Gab1 map to distinct regions (Figures 1E, 1F, and 2B–2D), allowing it to function as a scaffold that colocalizes these proteins and enhances PAR3 phosphorylation by PAR1 (Figure 3D). In addition, aPKC is brought into this Gab1 complex (Figure 2A). Gab1/aPKC

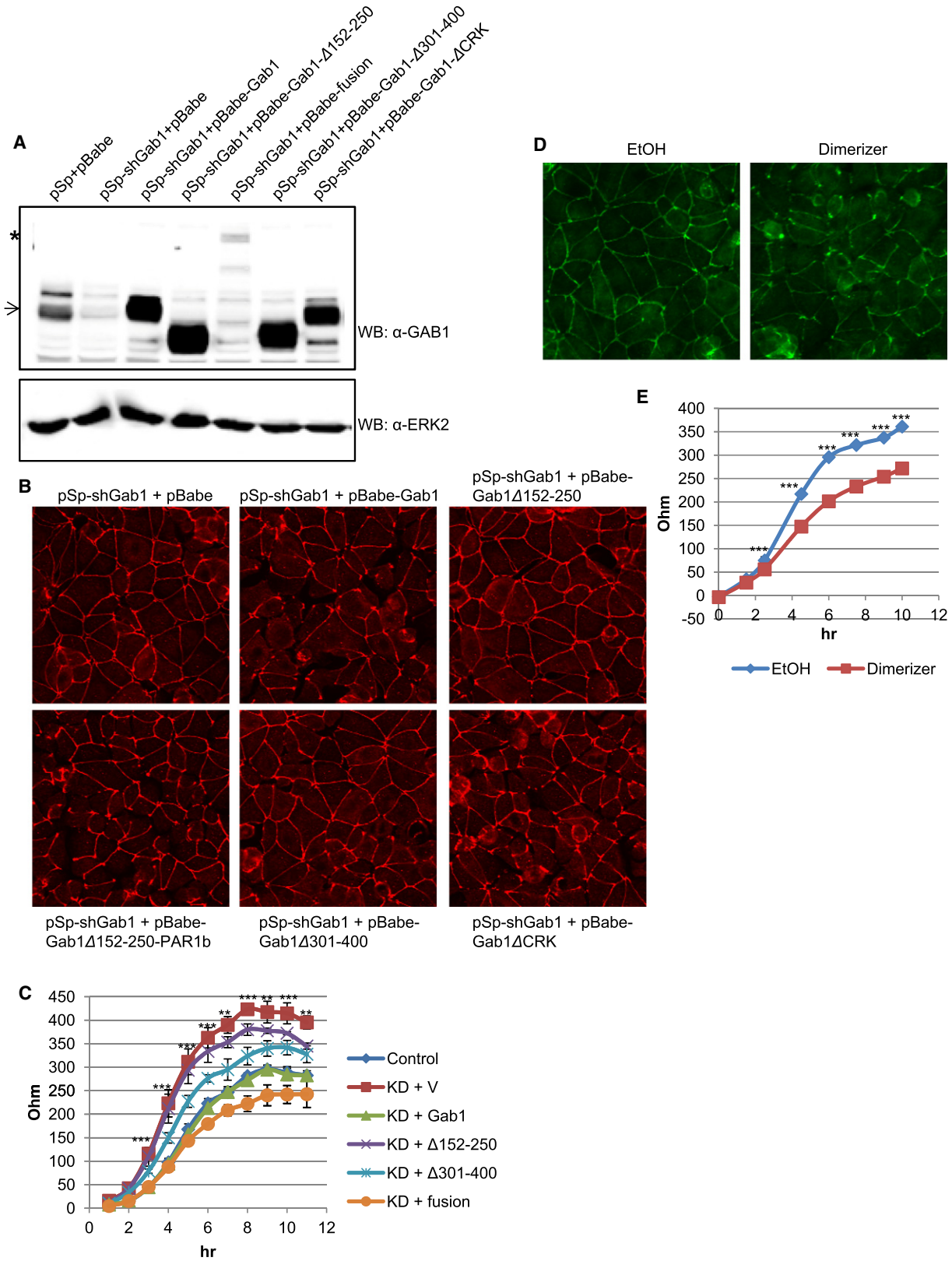
A
pSp+pBabe
pSp-shGab1+pBabe
pSp-shGab1+pBabe-Gab1
pSp-shGab1+pBabe-Gab1-Δ152-250
pSp-shGab1+pBabe-fusion
pSp-shGab1+pBabe-Gab1-Δ301-400
pSp-shGab1+pBabe-Gab1-ΔCRK
*
WB: α-GAB1
WB: α-ERK2
B
pSp-shGab1 + pBabe
pSp-shGab1 + pBabe-Gab1
pSp-shGab1 + pBabe-Gab1Δ152-250
pSp-shGab1 + pBabe-Gab1Δ152-250-PAR1b
pSp-shGab1 + pBabe-Gab1Δ301-400
pSp-shGab1 + pBabe-Gab1ΔCRK
C
Ohm
hr
Control
KD + V
KD + Gab1
KD + Δ152-250
KD + Δ301-400
KD + fusion
D
EtOH
Dimerizer
E
Ohm
hr
EtOH
Dimerizer

binding is mediated largely via PAR3 (Figures S2A and S2B), although we cannot exclude an additional, weak direct interaction with Gab1. By contrast, Gab1/PAR6 interaction is barely detectable (Figure 2A), because Gab1 and PAR6 each bind, in a mutually exclusive fashion, to the PAR3 PDZ1 domain (Figures 2E and 3H and Figure S2C).

Our results lead to a model in which GAB1 regulates the PAR3/aPKC/PAR6 complex in two ways (Figures 3D and 7C–7E). First, PAR1-catalyzed phosphorylation of PAR3 releases PAR3 from membranes, whereupon it is sequestered in the cytosol by 14-3-3 (PAR5) (McCaffrey and Macara, 2009). By enhancing PAR1 phosphorylation of PAR3 (Figure 3F), GAB1 promotes PAR3 release. GAB1/PAR3/aPKC interaction also prevents PAR3/aPKC/PAR6 complex formation, because GAB1 and PAR6 compete for PAR3 binding (Figure 3H). Hence, GAB1 facilitates mutual exclusion of PAR complexes (Macara, 2004a, 2004b) (see Introduction), negatively regulating TJ assembly and stability and apical-basal polarity (Figures 4–6). Conversely, in response to growth factor (e.g., HGF) stimulation, GAB1 accelerates junction breakdown, enhancing cell scattering (Figures 7A and 7B).

Multiple lines of evidence support this model. First, lowering *GAB1* levels in MDCK II cells leads to decreased phosphorylation of PAR3 (on its PAR1 sites) and increased levels of PAR3-PAR6-aPKC complex (Figures 3F and 3I). *PAR3*-KD MDCK II cells show delayed TJ formation in a calcium switch assay (Chen and Macara, 2005), whereas *GAB1*-KD cells, as predicted by our model, have the converse phenotype: accelerated recruitment of PAR3 to incipient TJs and precocious TJ formation (Figures 4A and 4B and Figure S4A). Re-expressing WT Gab1, but not Gab1 mutants lacking PAR1 or PAR3 binding, reverses this phenotype (Figures 5B and 5C). Furthermore, direct fusion of Gab1 lacking its PAR1 binding domain (Gab1Δ152-250) to PAR1b, or ligand-induced binding of PAR1b to such a mutant, restores Gab1 function (Figures 5B–5E). Finally, Gab1 localizes to lateral membranes, perfectly positioned to perform these functions (Figure 4D).

GAB1 also affects other aspects of polarity via PAR1. Lowering PAR1 levels or inhibiting its kinase activity causes shortening of the lateral membranes of MDCK II cells (Cohen et al., 2004; Suzuki et al., 2004). Consistent with our finding that Gab1 enhances PAR1 activity (Figure 3G), *GAB1*-KD MDCK II cells also have shortened lateral membranes (Figure 6A and Figure S6B). PAR1 has multiple substrates besides PAR3, including cytoskeleton-regulating proteins such as IRSp53, TAU, MAP2, and MAP4 (Benton and St Johnston, 2003; Cohen et al., 2011; Marx et al., 2010); which of these contribute(s) to determining the height of the lateral membrane remains to be elucidated. Conversely, GAB1 overexpression disrupts apical-basal polarity and causes multilumen cysts in 3D cultures (Figure 6). Notably, PAR3 depletion or PAR1b overexpression also leads to multilumen cysts (Bryant et al., 2010; Cohen et al., 2011; Hao et al., 2010). Finally, GAB1 enhances growth factor (e.g., HGF)-induced cell scattering. Previous studies showed that GAB1 must interact with SHP2 and Pak4 to mediate scattering (Paliouras et al., 2009); our studies now implicate GAB1/PAR1 and GAB1/PAR3 interactions in this process as well (Figure 7). Reconstituting *GAB1*-KD MDCK II cells with WT Gab1, but not mutants lacking either PAR1 (Gab1Δ152-250)- or PAR3 (Gab1Δ301-400)-binding sites, sensitizes MDCK II cells to HGF-induced scattering. Moreover, forced dimerization of Gab1Δ152-250 and PAR1 directly promotes scattering, implicating PAR1 as the key binding protein within the deleted region (152–250).

At first glance, our results appear to conflict with the ability of CagA (which inhibits PAR1) to evoke the "hummingbird phenotype" (which is essentially cell scattering) in gastric epithelial cells and its ability to promote spreading of TJ markers to the lateral membrane of MDCK-II cells (Saadat et al., 2007). One possible explanation for this discrepancy could be that overexpression of CagA completely inhibits PAR1 family members; by contrast, *GAB1* depletion decreases, but does not abolish, PAR1 activity. In addition, the CagA-induced "hummingbird phenotype" reportedly requires simultaneous inhibition of PAR1 and activation of SHP2 by CagA. Conversely, in our shRNA-mediated depletion and reconstitution experiments, we found that the Gab1/PAR1 complex positively regulates cell scattering. Saadat et al. transiently overexpressed PAR1b to explore its effects on CagA-induced scattering, which could have led to nonphysiological effects. By contrast, we studied stable MDCK II cell pools expressing PAR1b at endogenous levels (Figure 1D, left panel). Unlike Saadat et al., we found that induced interaction of a Gab1 mutant lacking its PAR1-binding site (Gab1Δ152-250) with PAR1b enhances HGF-induced scattering, whereas stable expression of PAR1 in WT, but not *GAB1*-depleted, cells delays TJ formation (Figure S4C). These data clearly indicate that PAR1 regulates TJ formation rate in a GAB1-dependent manner. Saadat et al. also found that PAR1b promotes CagA oligomerization, which is required to potentiate CagA binding to SHP2. Conceivably, PAR1b

Figure 5. GAB1 Regulates TJ Formation via the PAR Proteins

(A) Lysates from *GAB1*-KD MDCK II cells reconstituted with WT Gab1 or Gab1 mutants were immunoblotted, as indicated. Arrow indicates endogenous GAB1. * indicates Gab1Δ152-250-PAR1b fusion protein; note its low expression compared with endogenous GAB1.

(B) WT Gab1 and Gab1 mutant-reconstituted cells undergoing calcium switch were fixed 1 hr following Ca^{2+} repletion and stained with anti-ZO-1 antibodies. Representative confocal images are shown.

(C) TER (mean ± SD) was measured during calcium switch. "Controls" are parental MDCK II cells infected with retroviruses packaged with empty vectors of pBabe and pSuperior.retro.puro. **$p < 0.01$, ***$p < 0.001$, KD + V (or KD + Δ152-250 or KD + Δ301-400) versus KD + Gab1.

(D) *GAB1*-KD MDCK II cells stably expressing Gab1Δ152-250-FKBP and PAR1b-F*RB-HA were plated onto filters in S-MEM containing AP21697 or EtOH (vehicle) and subjected to calcium switch. One hour later, cells were fixed and immunostained with anti-ZO-1 antibodies. Representative confocal images are shown.

(E) Calcium switch assays on *GAB1*-KD MDCK II cells stably expressing Gab1Δ152-250-FKBP and PAR1b-F*RB-HA grown on filters in S-MEM in the presence of AP21697 or EtOH (vehicle) and TER (mean ± SD, ***$p < 0.001$) was monitored. Also, see Figure S5.

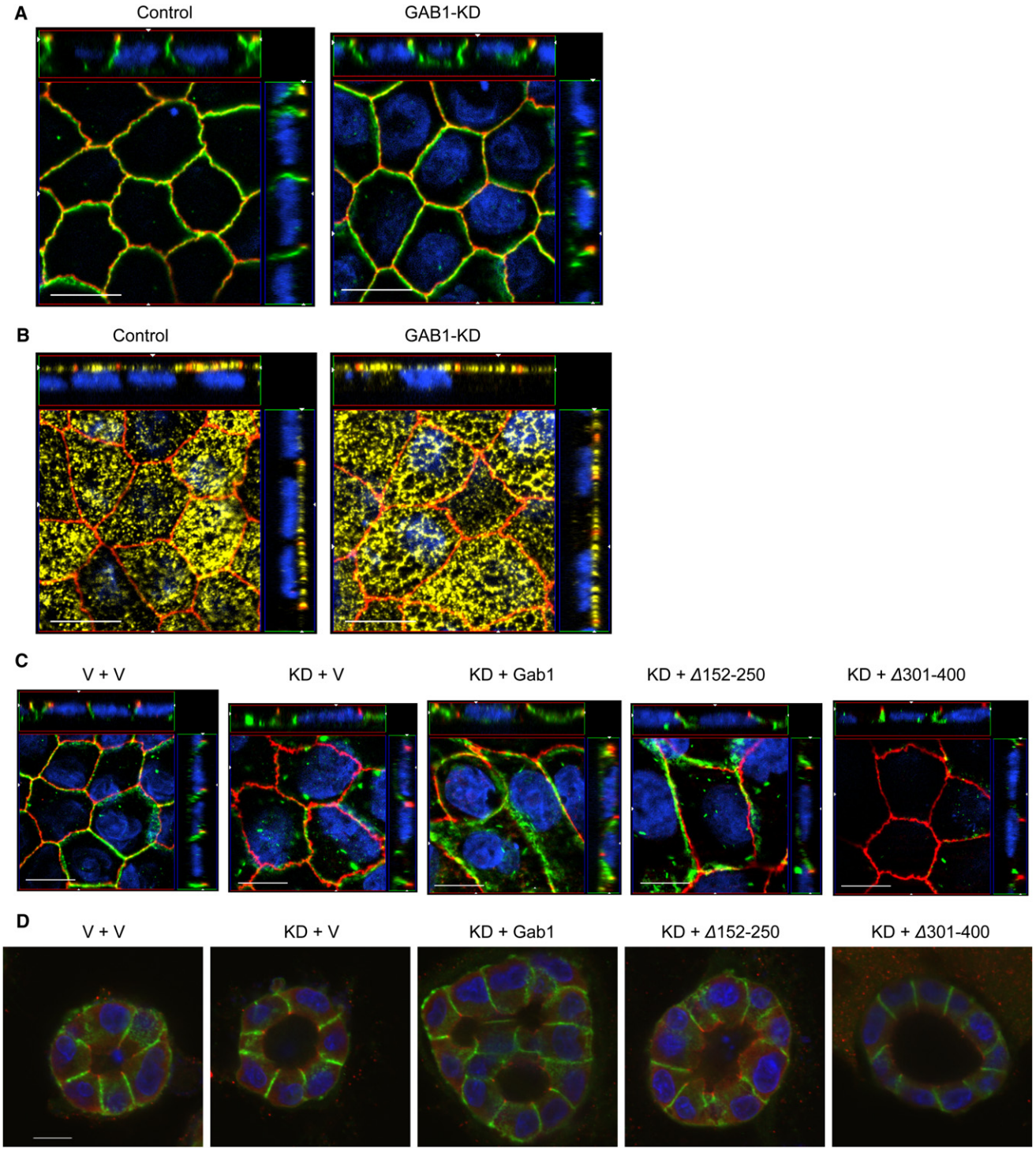

Figure 6. Gab1 Overexpression Disrupts Polarity

(A and B) Control and *GAB1*-KD MDCK II cells were cultured on filters for 3 days, then costained with anti-ZO-1 (red) and anti-E-cadherin (green) antibodies (A) or anti-ZO-1 (red) and anti-gp135 (yellow) antibodies (B).

(C) *GAB1*-KD MDCK II cells reconstituted with WT Gab1 or Gab1 mutants were cultured on filters for 3 days and then fixed and costained with anti-ZO-1 (red) and anti-E-cadherin (green) antibodies. Note disrupted polarity in WT Gab1-expressing cells.

(D) *GAB1*-KD MDCK II cells reconstituted with WT Gab1 or Gab1 mutants were cultured in Matrigel for 3 days. The resultant structures were costained with anti-ZO-1 (red) and anti-β-catenin (green) antibodies. Note that WT Gab1 (over)expressing cells form multilumen cysts in Matrigel. Scale bar, 10 μm. Also, see Figure S6.

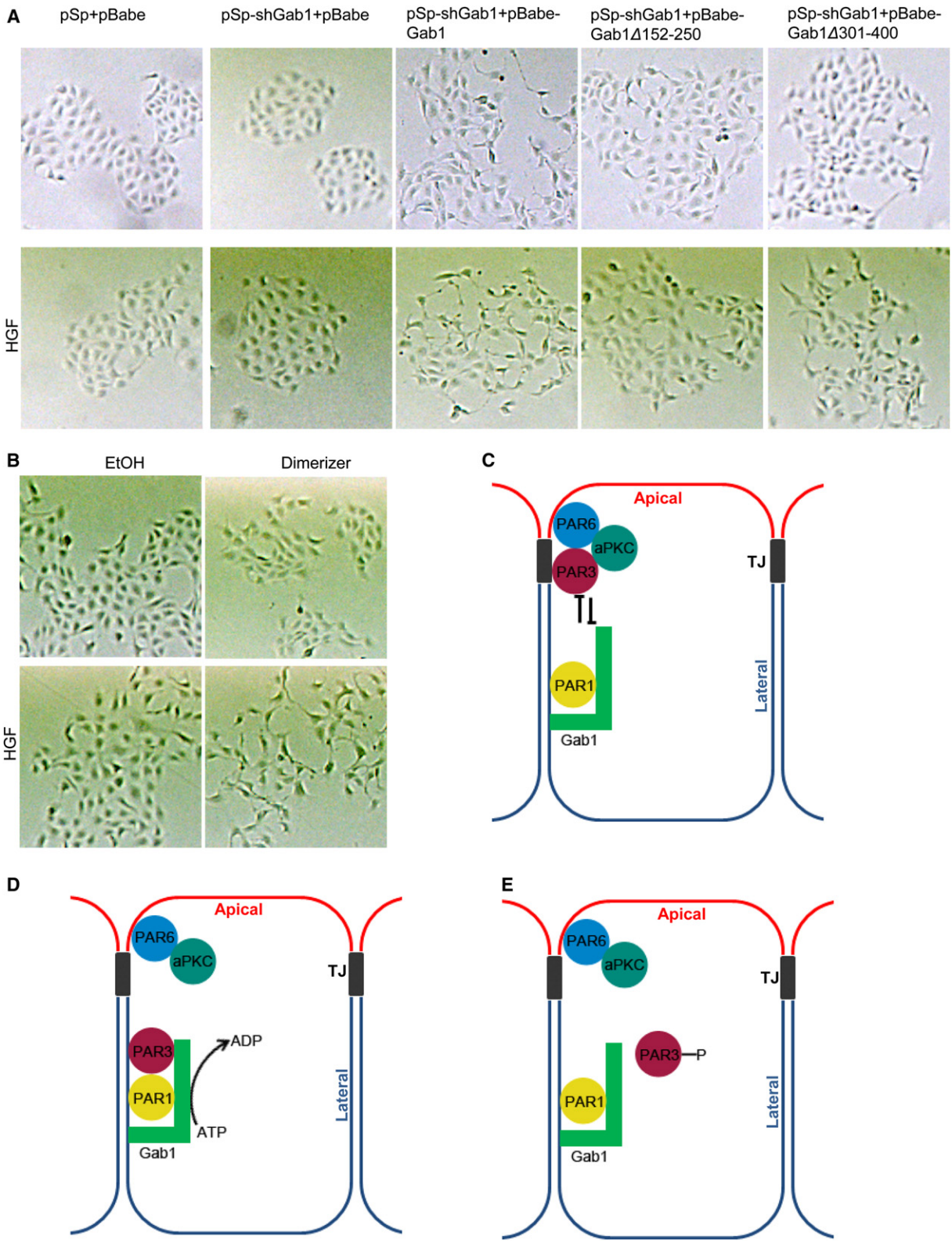

Figure 7. GAB1 Induces Cell Scattering via PAR1b/PAR3

(A) *GAB1*-KD MDCK II cells reconstituted with control vector or the indicated Gab1 constructs were starved in 0.2% FBS and then left untreated or stimulated with HGF (1 ng/ml). Note that WT Gab1-, but not Gab1Δ152-250- or Gab1Δ301-400-reconstituted, cells dissociated and adopted an elongated morphology.

activity must be inhibited to allow CagA oligomerization, in which case CagA could have evolved to inhibit PAR1 kinase activity.

Although our results show that they act differently from CagA, previous studies nonetheless implicate GAB proteins in oncogenesis. For example, *Gab1* is required for Met-induced transformation (Fixman et al., 1997; Mood et al., 2006). *GAB2* amplification/overexpression is implicated in melanoma cell migration and invasion (Horst et al., 2009), and *Gab2* is required for BCR/ABL-induced transformation (Sattler et al., 2002) and leukemogenesis (W. Chan, G. Mohi, S. Gu, S. Li, B.G.N., and R.V. Etten, unpublished data). *GAB2* overexpression promotes the proliferation and migration of MCF-10A breast epithelial cells, whereas coexpression of *GAB2* and *ErbB2/Neu* causes multiacinar structures and invasion (Bentires-Alj et al., 2006; Brummer et al., 2006). Transgenic *GAB2* overexpression enhances, whereas *Gab2* deletion impairs, *Neu*-evoked tumorigenesis, and *GAB2* is amplified in 10%–15% of human breast tumors (Bentires-Alj et al., 2006; Ke et al., 2007). The latter effects have been attributed to GAB2 actions in the RAS/ERK and RHOA pathways. However, ErbB2/Neu activation also causes disruption of the PAR3/PAR6/aPKC complex (Aranda et al., 2006), although the detailed mechanism has remained unclear. Our findings that ErbB2/Neu activation induces GAB1/PAR3 complex formation (Figure S2E) and that GAB1 negatively regulates TJ formation strongly implicate GAB proteins as key intermediaries in ErbB2/Neu effects on the polarity machinery. Ongoing studies should clarify the extent to which GAB/PAR protein complexes contribute to the oncogenic activity of GAB proteins.

EXPERIMENTAL PROCEDURES

Calcium Switch Assay

Calcium switch assays were performed as described (Cohen and Müsch, 2003). Briefly, cells were plated at high density onto 0.4 μm pore size Transwell filters (Corning) in Ca^{2+}-free Suspension-MEM (S-MEM, Sigma) with 10% dialyzed fetal bovine serum (FBS, GIBCOBRL) and cultured for 20 hr. Calcium switch was initiated by changing the media to S-MEM containing 1.8 mM Ca^{2+}.

Microscopy

Images were acquired using a Leica DFC 420 fluorescence microscope or an Olympus FluoView 1000 IX-81 laser scanning confocal microscope.

TER Measurements

Triplicate wells of MDCK II cells were plated at high density onto Transwell filters (12 mm, 0.4 μm pore size) in S-MEM. At various times after adding back Ca^{2+}, resistance across the monolayer was measured with a Millicell ERS Volt-Ohm meter (Millipore).

Cell Scattering

Cells were plated in MEM plus 10% FBS onto 6-well plates (15,000 cells/well), cultured for 2 days, and then starved in MEM containing 0.2% FBS with or without the AP21697 dimerizer for 6 hr, followed by treatment with 1 ng/ml HGF (PeproTech) for 18 hr. Images were acquired on a Leica DMI 3000 B microscope. Scattering was quantified by calculating the percentage of cells that dissociated and acquired elongated morphology.

Statistics

Data are presented as mean ± SD. Statistical significance was assessed using two-way ANOVA.

Detailed experimental procedures are provided in the Supplemental Information.

SUPPLEMENTAL INFORMATION

Supplemental Information includes seven figures and Supplemental Experimental Procedures and can be found with this article online at http://dx.doi.org/10.1016/j.molcel.2012.06.037.

ACKNOWLEDGMENTS

This work was supported by NIH grant R37 49152 to B.G.N., a grant from the Canadian Cancer Society Research Institute to M.I., grants CA098830 and BC075024, Era of Hope Scholar award from DOD Breast Cancer Research Program to S.K.M., and funding from the Princess Margaret Hospital Foundation and the Ontario Ministry of Health and Long Term Care. B.G.N. and M.I. are Canada Research Chairs, Tier 1; Z.Y. is the recipient of a postdoctoral fellowship from The Terry Fox Foundation; and M.U. received fellowships from The Uehara Memorial Foundation, The Naito Foundation, and the Terry Fox Foundation EIRR21 at CIHR. We thank Drs. T. Pawson (Samuel Lunenfeld Research Institute), M. Park (McGill University), I. Macara (University of Virginia), and H. Piwnica-Worms (Washington University Medical School) for constructs and Dr. G. Keller (Ontario Cancer Institute) for helpful comments.

Received: November 28, 2011
Revised: May 16, 2012
Accepted: June 18, 2012
Published online: August 9, 2012

REFERENCES

Aranda, V., Haire, T., Nolan, M.E., Calarco, J.P., Rosenberg, A.Z., Fawcett, J.P., Pawson, T., and Muthuswamy, S.K. (2006). Par6-aPKC uncouples ErbB2 induced disruption of polarized epithelial organization from proliferation control. Nat. Cell Biol. *8*, 1235–1245.

Bentires-Alj, M., Gil, S.G., Chan, R., Wang, Z.C., Wang, Y., Imanaka, N., Harris, L.N., Richardson, A., Neel, B.G., and Gu, H. (2006). A role for the scaffolding adapter GAB2 in breast cancer. Nat. Med. *12*, 114–121.

Benton, R., and St Johnston, D. (2003). Drosophila PAR-1 and 14-3-3 inhibit Bazooka/PAR-3 to establish complementary cortical domains in polarized cells. Cell *115*, 691–704.

Brummer, T., Schramek, D., Hayes, V.M., Bennett, H.L., Caldon, C.E., Musgrove, E.A., and Daly, R.J. (2006). Increased proliferation and altered growth factor dependence of human mammary epithelial cells overexpressing the Gab2 docking protein. J. Biol. Chem. *281*, 626–637.

Bryant, D.M., Datta, A., Rodríguez-Fraticelli, A.E., Peränen, J., Martín-Belmonte, F., and Mostov, K.E. (2010). A molecular network for de novo generation of the apical surface and lumen. Nat. Cell Biol. *12*, 1035–1045.

Chen, X., and Macara, I.G. (2005). Par-3 controls tight junction assembly through the Rac exchange factor Tiam1. Nat. Cell Biol. *7*, 262–269.

(B) *GAB1*-KD MDCK II cells stably expressing Gab1Δ152-250-FKBP and PAR1b-F*RB-HA were starved in 0.2% FBS containing AP21697 or EtOH (vehicle) and then left untreated or stimulated with 1 ng/ml HGF. Note that induced dimerization of Gab1Δ152-250-FKBP and PAR1b-F*RB sensitized cells to HGF-induced scattering.

(C–E) Role of GAB1 in regulating epithelial cell polarity: (C) In polarized epithelia, PAR3/PAR6/aPKC complex resides at the apical side of TJs (PAR6 and aPKC also localize to the apical domain), while PAR1 and Gab1 form a complex along the lateral membrane. Localization of these complexes is mutually exclusive. (D) PAR3 that "strays" from TJs and invades the lateral domain is "captured" by Gab1 and brought to PAR1 for phosphorylation. (E) Phosphorylated PAR3 is released from the Gab1/PAR1 complex into cytosol, where it can bind PAR5 (not shown). Also, see Figure S7.

Cohen, D., and Müsch, A. (2003). Apical surface formation in MDCK cells: regulation by the serine/threonine kinase EMK1. Methods *30*, 269–276.

Cohen, D., Brennwald, P.J., Rodriguez-Boulan, E., and Müsch, A. (2004). Mammalian PAR-1 determines epithelial lumen polarity by organizing the microtubule cytoskeleton. J. Cell Biol. *164*, 717–727.

Cohen, D., Fernandez, D., Lázaro-Diéguez, F., and Müsch, A. (2011). The serine/threonine kinase Par1b regulates epithelial lumen polarity via IRSp53-mediated cell-ECM signaling. J. Cell Biol. *192*, 525–540.

Cong, W., Hirose, T., Harita, Y., Yamashita, A., Mizuno, K., Hirano, H., and Ohno, S. (2010). ASPP2 regulates epithelial cell polarity through the PAR complex. Curr. Biol. *20*, 1408–1414.

Elbert, M., Rossi, G., and Brennwald, P. (2005). The yeast par-1 homologs kin1 and kin2 show genetic and physical interactions with components of the exocytic machinery. Mol. Biol. Cell *16*, 532–549.

Fixman, E.D., Holgado-Madruga, M., Nguyen, L., Kamikura, D.M., Fournier, T.M., Wong, A.J., and Park, M. (1997). Efficient cellular transformation by the Met oncoprotein requires a functional Grb2 binding site and correlates with phosphorylation of the Grb2-associated proteins, Cbl and Gab1. J. Biol. Chem. *272*, 20167–20172.

Gu, H., and Neel, B.G. (2003). The "Gab" in signal transduction. Trends Cell Biol. *13*, 122–130.

Hao, Y., Du, Q., Chen, X., Zheng, Z., Balsbaugh, J.L., Maitra, S., Shabanowitz, J., Hunt, D.F., and Macara, I.G. (2010). Par3 controls epithelial spindle orientation by aPKC-mediated phosphorylation of apical Pins. Curr. Biol. *20*, 1809–1818.

Hatakeyama, M. (2003). Helicobacter pylori CagA—a potential bacterial oncoprotein that functionally mimics the mammalian Gab family of adaptor proteins. Microbes Infect. *5*, 143–150.

Hatakeyama, M. (2004). Oncogenic mechanisms of the Helicobacter pylori CagA protein. Nat. Rev. Cancer *4*, 688–694.

Hirose, T., Karasawa, M., Sugitani, Y., Fujisawa, M., Akimoto, K., Ohno, S., and Noda, T. (2006). PAR3 is essential for cyst-mediated epicardial development by establishing apical cortical domains. Development *133*, 1389–1398.

Horst, B., Gruvberger-Saal, S.K., Hopkins, B.D., Bordone, L., Yang, Y., Chernoff, K.A., Uzoma, I., Schwipper, V., Liebau, J., Nowak, N.J., et al. (2009). Gab2-mediated signaling promotes melanoma metastasis. Am. J. Pathol. *174*, 1524–1533.

Hurd, T.W., Fan, S., Liu, C.J., Kweon, H.K., Hakansson, K., and Margolis, B. (2003). Phosphorylation-dependent binding of 14-3-3 to the polarity protein Par3 regulates cell polarity in mammalian epithelia. Curr. Biol. *13*, 2082–2090.

Hurov, J.B., Stappenbeck, T.S., Zmasek, C.M., White, L.S., Ranganath, S.H., Russell, J.H., Chan, A.C., Murphy, K.M., and Piwnica-Worms, H. (2001). Immune system dysfunction and autoimmune disease in mice lacking Emk (Par-1) protein kinase. Mol. Cell. Biol. *21*, 3206–3219.

Hurov, J.B., Huang, M., White, L.S., Lennerz, J., Choi, C.S., Cho, Y.R., Kim, H.J., Prior, J.L., Piwnica-Worms, D., Cantley, L.C., et al. (2007). Loss of the Par-1b/MARK2 polarity kinase leads to increased metabolic rate, decreased adiposity, and insulin hypersensitivity in vivo. Proc. Natl. Acad. Sci. USA *104*, 5680–5685.

Itoh, M., Yoshida, Y., Nishida, K., Narimatsu, M., Hibi, M., and Hirano, T. (2000). Role of Gab1 in heart, placenta, and skin development and growth factor- and cytokine-induced extracellular signal-regulated kinase mitogen-activated protein kinase activation. Mol. Cell. Biol. *20*, 3695–3704.

Ke, Y., Wu, D., Princen, F., Nguyen, T., Pang, Y., Lesperance, J., Muller, W.J., Oshima, R.G., and Feng, G.S. (2007). Role of Gab2 in mammary tumorigenesis and metastasis. Oncogene *26*, 4951–4960.

Kemphues, K. (2000). PARsing embryonic polarity. Cell *101*, 345–348.

Lee, H.S., Nishanian, T.G., Mood, K., Bong, Y.S., and Daar, I.O. (2008). EphrinB1 controls cell-cell junctions through the Par polarity complex. Nat. Cell Biol. *10*, 979–986.

Lennerz, J.K., Hurov, J.B., White, L.S., Lewandowski, K.T., Prior, J.L., Planer, G.J., Gereau, R.W., 4th, Piwnica-Worms, D., Schmidt, R.E., and Piwnica-Worms, H. (2010). Loss of Par-1a/MARK3/C-TAK1 kinase leads to reduced adiposity, resistance to hepatic steatosis, and defective gluconeogenesis. Mol. Cell. Biol. *30*, 5043–5056.

Macara, I.G. (2004a). Par proteins: partners in polarization. Curr. Biol. *14*, R160–R162.

Macara, I.G. (2004b). Parsing the polarity code. Nat. Rev. Mol. Cell Biol. *5*, 220–231.

Maroun, C.R., Holgado-Madruga, M., Royal, I., Naujokas, M.A., Fournier, T.M., Wong, A.J., and Park, M. (1999). The Gab1 PH domain is required for localization of Gab1 at sites of cell-cell contact and epithelial morphogenesis downstream from the met receptor tyrosine kinase. Mol. Cell. Biol. *19*, 1784–1799.

Maroun, C.R., Naujokas, M.A., Holgado-Madruga, M., Wong, A.J., and Park, M. (2000). The tyrosine phosphatase SHP-2 is required for sustained activation of extracellular signal-regulated kinase and epithelial morphogenesis downstream from the met receptor tyrosine kinase. Mol. Cell. Biol. *20*, 8513–8525.

Marx, A., Nugoor, C., Panneerselvam, S., and Mandelkow, E. (2010). Structure and function of polarity-inducing kinase family MARK/Par-1 within the branch of AMPK/Snf1-related kinases. FASEB J. *24*, 1637–1648.

McCaffrey, L.M., and Macara, I.G. (2009). Widely conserved signaling pathways in the establishment of cell polarity. Cold Spring Harb. Perspect. Biol. *1*, a001370.

Mood, K., Saucier, C., Bong, Y.S., Lee, H.S., Park, M., and Daar, I.O. (2006). Gab1 is required for cell cycle transition, cell proliferation, and transformation induced by an oncogenic met receptor. Mol. Biol. Cell *17*, 3717–3728.

Morais-de-Sá, E., Mirouse, V., and St Johnston, D. (2010). aPKC phosphorylation of Bazooka defines the apical/lateral border in Drosophila epithelial cells. Cell *141*, 509–523.

Paliouras, G.N., Naujokas, M.A., and Park, M. (2009). Pak4, a novel Gab1 binding partner, modulates cell migration and invasion by the Met receptor. Mol. Cell. Biol. *29*, 3018–3032.

Rosário, M., and Birchmeier, W. (2003). How to make tubes: signaling by the Met receptor tyrosine kinase. Trends Cell Biol. *13*, 328–335.

Saadat, I., Higashi, H., Obuse, C., Umeda, M., Murata-Kamiya, N., Saito, Y., Lu, H., Ohnishi, N., Azuma, T., Suzuki, A., et al. (2007). Helicobacter pylori CagA targets PAR1/MARK kinase to disrupt epithelial cell polarity. Nature *447*, 330–333.

Sachs, M., Brohmann, H., Zechner, D., Müller, T., Hülsken, J., Walther, I., Schaeper, U., Birchmeier, C., and Birchmeier, W. (2000). Essential role of Gab1 for signaling by the c-Met receptor in vivo. J. Cell Biol. *150*, 1375–1384.

Sattler, M., Mohi, M.G., Pride, Y.B., Quinnan, L.R., Malouf, N.A., Podar, K., Gesbert, F., Iwasaki, H., Li, S., Van Etten, R.A., et al. (2002). Critical role for Gab2 in transformation by BCR/ABL. Cancer Cell *1*, 479–492.

Sottocornola, R., Royer, C., Vives, V., Tordella, L., Zhong, S., Wang, Y., Ratnayaka, I., Shipman, M., Cheung, A., Gaston-Massuet, C., et al. (2010). ASPP2 binds Par-3 and controls the polarity and proliferation of neural progenitors during CNS development. Dev. Cell *19*, 126–137.

Suzuki, A., and Ohno, S. (2006). The PAR-aPKC system: lessons in polarity. J. Cell Sci. *119*, 979–987.

Suzuki, A., Hirata, M., Kamimura, K., Maniwa, R., Yamanaka, T., Mizuno, K., Kishikawa, M., Hirose, H., Amano, Y., Izumi, N., et al. (2004). aPKC acts upstream of PAR-1b in both the establishment and maintenance of mammalian epithelial polarity. Curr. Biol. *14*, 1425–1435.

Wöhrle, F.U., Daly, R.J., and Brummer, T. (2009). Function, regulation and pathological roles of the Gab/DOS docking proteins. Cell Commun. Signal. *7*, 22.